

Available online at www.sciencedirect.com

ScienceDirect

Procedia IUTAM 14 (2015) 152 – 162

Procedia
IUTAM

www.elsevier.com/locate/procedia

IUTAM_ABCM Symposium on Laminar Turbulent Transition

Experimental investigation of the effect of forward-facing steps on boundary layer transition

Marco Costantini^{a,*}, Steffen Risius^a, Christian Klein^a^aDeutsches Zentrum für Luft- und Raumfahrt e.V. (DLR), Göttingen D-37073, Germany

Abstract

The effect of geometric forward-facing steps on boundary layer transition was experimentally investigated at a high subsonic Mach number in a blow-down wind tunnel facility in Göttingen, Germany. Boundary layer transition was detected non-intrusively by means of the Temperature-Sensitive Paint (TSP) technique. Forward-facing steps of different height were installed on a spanwise invariant wind tunnel model. Streamwise pressure gradient and high chord Reynolds number were systematically varied and their effect on boundary layer transition was studied in the presence of forward-facing steps on the model surface. At all tested stability situations, the surface imperfections were shown to reduce the extent of the laminar region. Transition was observed to move gradually towards the step location with increasing step Reynolds numbers and increasing relative step height. For a given combination of step height and chord Reynolds number, more pronounced negative pressure gradients led to an increase in transition Reynolds number. The reduction in transition Reynolds number due to the effect of the surface imperfection was more marked at larger flow acceleration. The plots of the relative change in transition location as a function of the step Reynolds number and of the relative step height gave good correlation of the results. The correlations were found to be practically independent of the streamwise pressure gradient in the examined range. Criteria for the allowable tolerances on low-sweep Natural Laminar Flow surfaces can now be derived from the functional relations determined in this work.

© 2015 The Authors. Published by Elsevier B.V. This is an open access article under the CC BY-NC-ND license (<http://creativecommons.org/licenses/by-nc-nd/4.0/>).

Selection and peer-review under responsibility of ABCM (Brazilian Society of Mechanical Sciences and Engineering)

Keywords: Boundary layer transition; forward-facing steps; Temperature-Sensitive Paint; TSP

* Corresponding author. Tel.: +49-551-709-2632; fax: +49-551-709-2830.

E-mail address: marco.costantini@dlr.de

1. Introduction

Modern manufacturing techniques for metallic and composite materials can provide surface smoothness suitable for Natural Laminar Flow (NLF), but surface imperfections, such as steps and gaps at junctions, waviness, and bulges, can still affect the behavior of the boundary layer on aircraft surfaces^{1,2}. Therefore, manufacturing tolerances must be specified for the shape and dimension of these imperfections in order to ensure achievement of laminar flow, thus maintaining the advantages of NLF in terms of drag reduction^{1,2}. This can be done only after the quantification of the effects of surface imperfections on the stability of the laminar boundary layer^{1,3}. Past research on specific surface geometries at selected flow conditions supplied criteria to predict the effect of surface imperfections on boundary layer transition^{4,5}. However, the considered boundary layer stability situations were not taken into account in the formulation of the criteria, so that they can be applied only to specific cases. In the last decades, efforts were put into the understanding of the physics involving imperfection-induced transition and into the development of models and criteria for predicting the effect of surface imperfections on the laminar boundary layer^{1,3,6-14}. Although many improvements have been carried out in this field, there are still no universal criteria available covering a wide range of stability situations. In particular, there were no studies examining systematically the effect of sharp forward-facing steps (FFS) on boundary layer transition for compressible flow at both zero and favorable streamwise pressure gradients. These investigations have been conducted in this work. Natural Laminar Flow has been demonstrated to be attainable on surfaces at low sweep angles^{15,16}, where the main mechanism leading to transition to turbulence is the growth of Tollmien-Schlichting instabilities^{15,17}. Therefore, the present work focuses on the effect of forward-facing steps on two-dimensional flow.

Surface steps can originate from the installation of leading edge panels on wings, nacelles and control surfaces and from the installation of access panels, doors, and windows on fuselage noses and engine nacelles^{1,2}. The numerical computation of the flowfield over a forward-facing step is still resource-intensive^{2,3,12}, so that a parametric study of the effect of the step on boundary layer transition is typically performed only for a selected configuration and a limited variation of flow conditions^{3,12}.

In this work, spanwise invariant forward-facing steps, perpendicular to a (quasi) two-dimensional flow, were experimentally investigated at a high subsonic Mach number in the wind tunnel facility DNW-KRG^{18,19}. The effects on boundary layer transition of forward-facing steps, Reynolds number, and streamwise pressure gradient, were studied using the newly designed *PaLASTra* model²⁰.

2. Experimental setup and definition of parameters

The tests were conducted in the Cryogenic Ludwig-Tube Göttingen (DNW-KRG)¹⁸, a low-turbulence ($Tu_{pu} \sim 0.06\%$ ¹⁹), intermittently operating wind tunnel facility capable of achieving flight Reynolds and Mach numbers of a transonic commercial aircraft by increasing the pressure and decreasing the temperature of gaseous nitrogen, which is used as the test gas. The DNW-KRG test section has adaptive upper and lower walls that allow interference-free contours to be set¹⁸. The inflow Reynolds and Mach number are determined from the inflow pressure and temperature measurements^{18,19}; the uncertainties in the present work were within $\Delta Re = \pm 0.05$ Mio. and $\Delta M = \pm 0.002$. By virtue of the working principle of the DNW-KRG blow-down facility, a temperature difference between flow and model surface occurs during a run after the flow temperature has dropped due to the gas expansion¹⁸. Therefore, the model surface temperature T_w is generally larger than the adiabatic wall temperature T_{aw} . For attached two-dimensional flows, $T_w/T_{aw} > 1$ enhances boundary layer instability and can cause transition to occur earlier than in the adiabatic case^{20,23}. On the other hand, the temperature difference between flow and model surface enables very accurate transition detection using the Temperature-Sensitive Paint (TSP) measurement technique^{24,25} at DNW-KRG^{20,23,25,26}. The custom-built design of the DNW-KRG facility and a special method for model handling and cleaning guarantee operation with clean flow conditions, which is crucial for NLF testing at high Reynolds numbers. At such test conditions, even micron-sized dust particles impacting onto or adhering to the model leading edge can cause premature transition and thereby make detection of natural transition very difficult or even impossible^{26,27}.

The *PaLASTra* two-dimensional wind tunnel model²⁰ was designed for the systematic study of the effect on boundary layer transition of two-dimensional surface imperfections, changes in Reynolds number, Mach number,

and streamwise pressure gradient, and the effect of a non-adiabatic wing surface. The shape adopted for the airfoil is shown in cross section in Fig. 1a. A flat surface was designed for the largest part of the upper side of the model, which was the one of main interest in this work: in this manner the pressure gradient was practically uniform on a large portion of the model upper surface (approx. $20\% < x/c < 70\%$). The wind tunnel model was made from austenitic stainless steel. Two-dimensional steps (uniform in spanwise direction) of a desired height could be mounted at the chordwise location $x_h/c = 35\%$ by installing shims of appropriate thickness at the interface between the two parts comprising the model (see Fig. 1a). The shape of the imperfection (abrupt step with sharp edges) was thus assured to be the same for each tested configuration. The spanwise non-uniformity of the step was within $\pm 1\ \mu\text{m}$, measured using a contact profilometer with a vertical resolution of $\pm 0.8\ \text{nm}$.

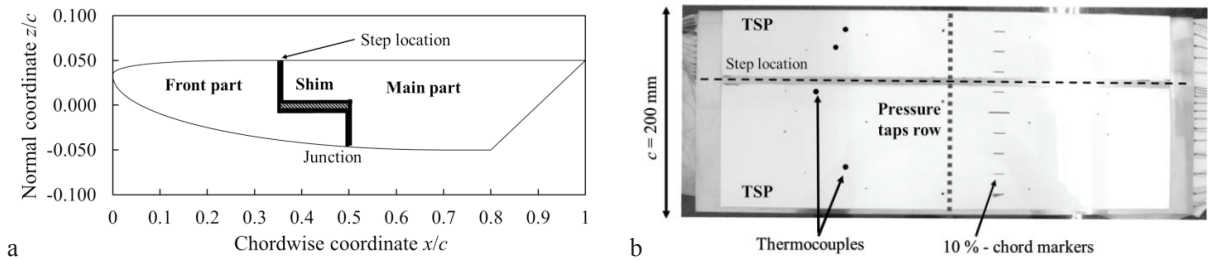


Fig. 1. *PaLASTra* model¹⁵. a: side view (cross section): *PaLASTra* airfoil and sketch of the model construction for the installation of steps; b: top view and instrumentation (leading edge on top of the image).

As shown in Fig. 1b, the *PaLASTra* model was coated with Temperature-Sensitive Paint (TSP)^{21,22} for non-intrusive transition detection and equipped with pressure taps for measuring the pressure distribution and thermocouples for monitoring the model temperature evolution during a test run²⁰. The TSP was applied in pockets machined into the model surface, so that the final model contour did not present variations from the designed contour. As it can be seen in Fig. 1b, a strip of width $\Delta x/c = 5\%$ about the step location was left uncoated: the sharpness of the step was thus ensured by creating it between two metallic surfaces. TSP formulation, surface quality, optical setup, acquisition and elaboration of the TSP images were the same as those discussed in Ref. 20. The uncertainty in the transition location was within $\Delta x_T/c = \pm 2\%$ (less than $\Delta x_T/c = \pm 1\%$ for the majority of the cases). The uncertainty in the wall temperature measurements and in the evaluated pressure coefficients on the model surface was within $\Delta T_w = \pm 0.3\ \text{K}$ and $\Delta c_p = \pm 0.005$.

The described experimental setup allowed Mach number, Reynolds number, streamwise pressure gradient, wall temperature ratio, and step height to be changed independently of each other, which was essential for the present study. The Mach number M used in this work is the ratio of velocity and speed of sound of the freestream. The Reynolds number Re is based on the model chord length $c = 0.2\ \text{m}$, on the freestream velocity and on the freestream kinematic viscosity. The Hartree parameter β_H of the Falkner-Skan family of self-similar boundary layers and the wall temperature ratio T_w/T_{aw} were chosen as the characteristic parameters for the pressure distribution and for the thermal boundary condition at the model surface, respectively. The Hartree parameter β_H , defined as in Ref. 28, was evaluated for each test run with the smooth configuration as the average value on the chordwise portion where the pressure gradient was practically uniform. The uncertainty in the Hartree parameter was within $\Delta\beta_H = \pm 0.002$. T_w is the model surface temperature corresponding to the laminar boundary layer, evaluated as the average of the measurements of the two thermocouples located at the two more upstream positions $x/c = 10\%$ and 20% . T_{aw} is the adiabatic wall temperature computed at $x/c = 15\%$. The evaluated uncertainty in the wall temperature ratio was within $\Delta(T_w/T_{aw}) = \pm 0.002$. The boundary layer displacement thickness δ_1 , used later in this work, was calculated using the boundary layer solver COCO²⁹, modified for calculations with isothermal wall³⁰. A uniform temperature equal to T_w was imposed at the model surface.

3. Results and discussion

The tests were focused on the influence of streamwise pressure gradient and forward-facing steps on boundary layer transition. For all test conditions, the model and the gas in the DNW-KRG storage tube were set at approximately the same temperature before the run $T \sim 288$ K. The tests were conducted at standard DNW-KRG thermal conditions at the model surface: $T_w/T_{aw} \sim 1.045$ - 1.065 for the cases considered in the present work. The thermal condition at the model surface was approximately the same for all configurations, with and without steps installed, so that the influence of T_w/T_{aw} on the following results could be generally minimized. The test Mach number was $M = 0.77$, which is in the range of typical Mach numbers for cruise conditions of a civil commercial aircraft with NLF surfaces¹⁵⁻¹⁷. The investigations were conducted at chord Reynolds numbers $4 \text{ Mio.} \leq Re \leq 13 \text{ Mio.}$ and at streamwise pressure gradients $0.005 \leq \beta_H \leq 0.112$; this variation of parameters covers a considerable range of flight conditions of NLF surfaces^{1-9-11,15-17,31}. Forward-facing steps of height $h = 29, 60, \text{ and } 89 \mu\text{m}$ were installed on the model upper side.

The effect of the forward-facing steps at $\beta_H = 0.066$ is shown with the TSP results in Fig. 2 for a Reynolds number $Re = 6 \text{ Mio.}$ Even the smallest forward-facing step of height $h = 29 \mu\text{m}$ made the laminar boundary layer more unstable and led to a displacement of the transition location to a more upstream position: from $x_{T,0}/c \sim 75 \%$ for the smooth configuration (no steps installed, subscript “0”) to $x_T/c \sim 65 \%$ with a forward-facing step of height $h = 29 \mu\text{m}$. The steps of approximately double and triple this height caused a further displacement of the transition location towards a more upstream position, up to $x_T/c \sim 47 \%$ with the step of height $h = 89 \mu\text{m}$. The model surface pressure coefficients c_p measured for the four configurations are plotted in Fig. 3 as a function of the chordwise coordinate. A glance at Fig. 3a shows that the presence of the surface imperfection had a negligible effect on the pressure distributions, except the region around the step location. A zoomed-in plot of this area is presented in Fig. 3b. It can be seen that the imperfection began to influence the flow evolution from $x/c \sim 29 \%$. With respect to the smooth configuration, and proceeding in the streamwise direction, the boundary layer was decelerated upstream of the step, accelerated over the step, and decelerated again downstream of the step. Larger differences from the base flow were observed for configurations with higher steps. The pressure distribution of the smooth configuration was recovered at $x/c > 40 \%$, the exact location being more downstream with increasing step height.

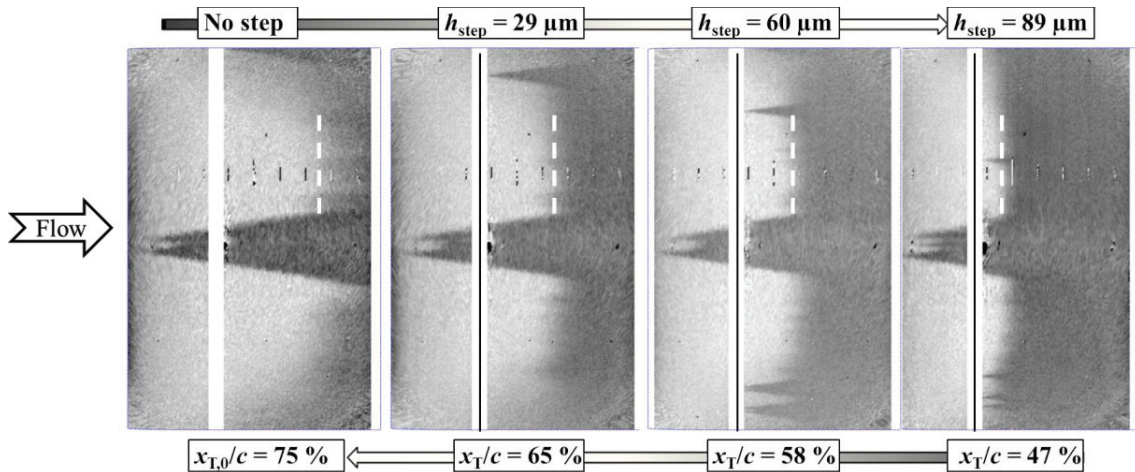


Fig. 2. TSP results at $Re = 6 \text{ Mio.}$, $M = 0.77$, $\beta_H = 0.066$, and $T_w/T_{aw} \sim 1.05$. Bright and dark areas are laminar and turbulent regions, respectively. The detected transition location is indicated by the dashed white line, with the step location being shown by the black solid line. The whitened strips correspond to the metallic surfaces of the model where no paint had been applied. The two turbulent wedges in the mid-span domain arose from pressure taps in the leading edge region; the other turbulent wedges were caused by contamination of the model surface at the step location.

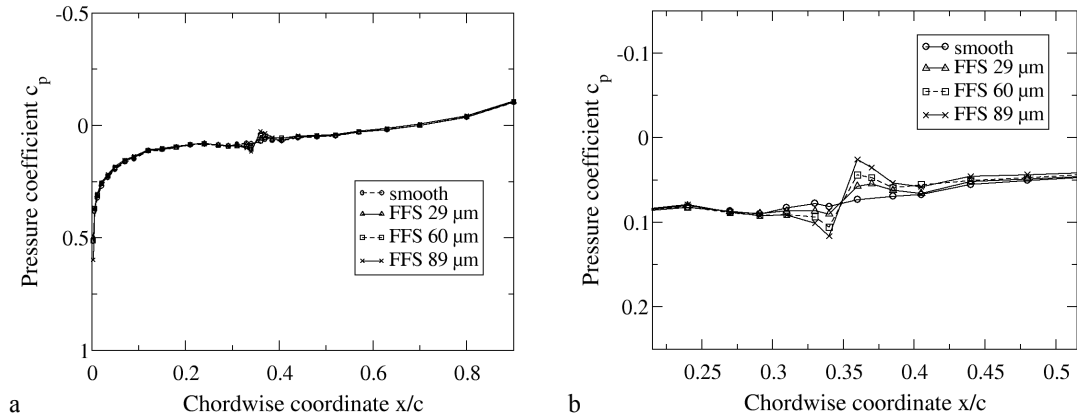


Fig. 3. Measured pressure distributions at $Re = 6 \text{ Mio.}$, $M = 0.77$, $\beta_H = 0.066$, and $T_v/T_{aw} \sim 1.05$. Smooth configuration (no step) and configurations with forward-facing steps installed. (a) overview; (b) zoomed-in of left figure in proximity of the step location.

These effects of the forward-facing steps were observed also for all other combinations of streamwise pressure gradient and chord Reynolds number. A comparison of the results obtained at two different pressure gradients is presented in Fig. 4. The upper two and the lower two TSP results were obtained at $\beta_H = 0.036$ and 0.063 , respectively. The TSP results achieved for a smooth configuration, Figs. 4a and 4d, can be compared at first: as expected, the effect of larger flow acceleration in the absence of surface imperfections was to delay transition²⁰⁻²². A favorable effect of larger Hartree parameter was found also in the presence of forward-facing steps, as it can be seen by the comparison of the TSP results obtained at $h = 60 \mu\text{m}$ and presented in Figs. 4b and 4e. Nevertheless, it should be noted here also that the shift in transition location (in both absolute and relative terms) due to the effect of the surface imperfection was more marked for the case at larger Hartree parameter. This result is related to the increased sensitivity of transition to the considered forward-facing steps, as qualitatively shown in Figs. 4c and 4f, where the results of linear stability computations are plotted. Linear stability analysis of the smooth configuration boundary layer was carried out by means of LILO³². The amplification factors of the disturbances superimposed upon the laminar boundary layer (N -factors) were calculated using compressible stability theory without curvature effects. The N -factors were computed for waves with fixed propagation direction and different frequencies (constant wave angle strategy). The propagation direction was fixed to zero degrees because the maximum amplification rate is that of two-dimensional waves up to a Mach number of approx. 0.9^9 . Transition occurred for $\beta_H = 0.036$ at $x_{T,0}/c = 44 \%$, on a region where the slope of the envelope curve of the amplification factors (N -factors) is positive, see Fig. 4c. The larger flow acceleration at $\beta_H = 0.063$ damped the amplification of the disturbances and delayed transition to $x_{T,0}/c = 69 \%$, where $\partial N_{x_{T,0}}/\partial(x/c) \sim 0$ (Fig. 4f). Following the procedure described in Refs. 6, 8, and 33, transition was assumed to occur when a threshold amplification ratio $e^{N_T} = e^{N_{T,0}}$, independent of the presence of the imperfections, has been reached; the effect of the step was modelled as an increment ΔN to be added to the N -factor envelope curve of the smooth configuration. It can be seen in Figs. 4c and 4f that the movement of the transition location – predicted using the modified N -factor envelope curve according to the aforementioned procedure – is more pronounced for the case where $\partial N_{x_{T,0}}/\partial(x/c)$ was approx. zero ($\beta_H = 0.063$) rather than that for the case where $\partial N_{x_{T,0}}/\partial(x/c) > 0$ ($\beta_H = 0.036$). This is in agreement with the behavior observed in the present experiment. (Note that the increment ΔN in Figs. 4c and 4f is qualitative and was used only for explanatory purposes. A constant $\Delta N \sim h/\delta_{1,8}$ has been assumed, but also a variable ΔN_6 would have led to the same conclusion.)

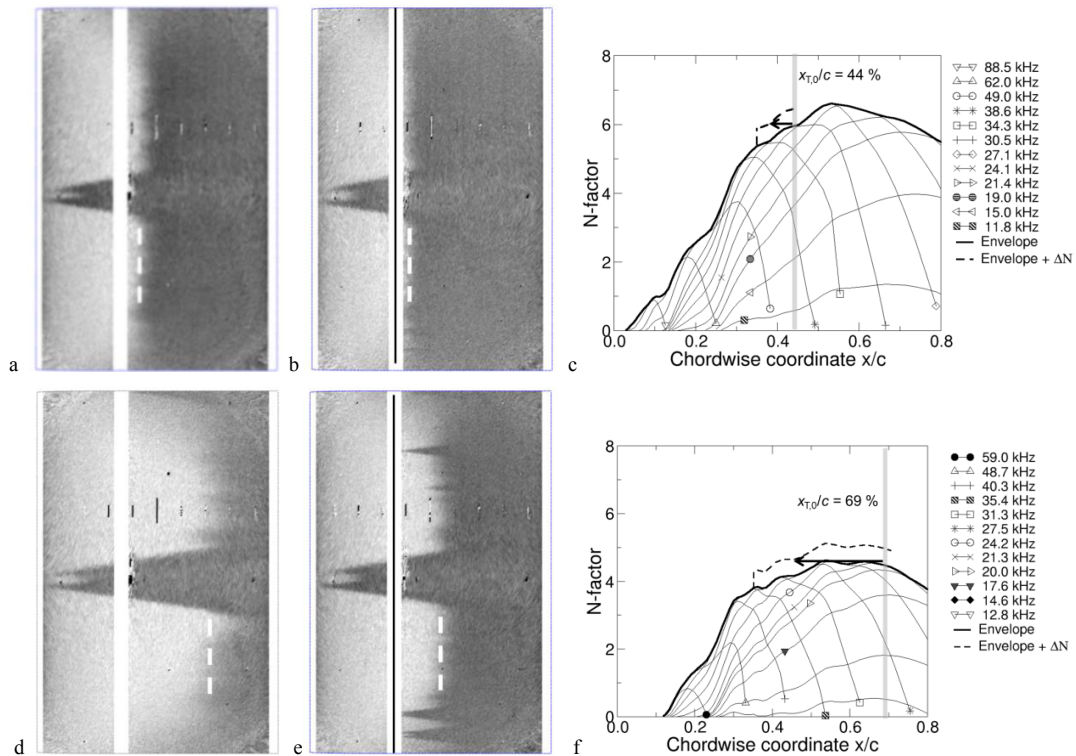


Fig. 4. $Re = 6 \text{ Mio.}$, $M = 0.77$, and $T_w/T_{aw} \sim 1.05$. Upper figures: $\beta_H = 0.036$. a: TSP result, no step; $x_{T,0}/c = 44\%$. b: TSP result, $h = 60 \mu\text{m}$; $x_T/c = 40\%$. c: results of linear stability analysis. Bottom figures: $\beta_H = 0.063$. d: TSP result, no step; $x_{T,0}/c = 69\%$. e: TSP result, $h = 60 \mu\text{m}$; $x_T/c = 54\%$. f: results of linear stability analysis. Amplification rates shown only for a few frequencies. The linear stability computations were carried out for the smooth configuration; the step disturbance was (qualitatively) modelled as a constant increment ΔN_8 . The transition location $x_{T,0}/c$ measured on the smooth configuration is shown by a grey bar. The predicted transition movement (qualitative), due to the step disturbance, is shown by a black arrow.

The results for all tested conditions are brought together in Fig. 5, where the transition Reynolds number Re_{xT} (based on freestream velocity, freestream kinematic viscosity and laminar run length $x_{T,0}$ or x_T) is plotted as a function of the pressure gradient parameter β_H . Only a few representative error bars for the results are actually plotted in this and in the following figures. At fixed streamwise pressure gradient, the negative effect of higher forward-facing steps on Re_{xT} can clearly be seen in Fig. 5. The positive influence of more pronounced flow acceleration on boundary layer transition is also apparent in Fig. 5: this effect was observed not only for the smooth configuration, as expected²⁰⁻²², but also confirmed in the presence of forward-facing steps. The favorable influence of a larger Hartree parameter on the transition Reynolds number is however less marked as the step height increases, leading to smaller increases of Re_{xT} with larger step heights for the same change in β_H . As a result of the increased sensitivity of boundary layer transition at more pronounced streamwise pressure gradients, the reduction in Re_{xT} due to the effect of the steps is larger at larger Hartree parameters. Note also that the transition Reynolds number appears to be practically independent of the chord Reynolds number: this can be seen not only for the results obtained with the smooth configuration, as expected for this model designed for an approximately uniform pressure gradient in the streamwise direction²⁰⁻²², but also for those with installed forward-facing steps.

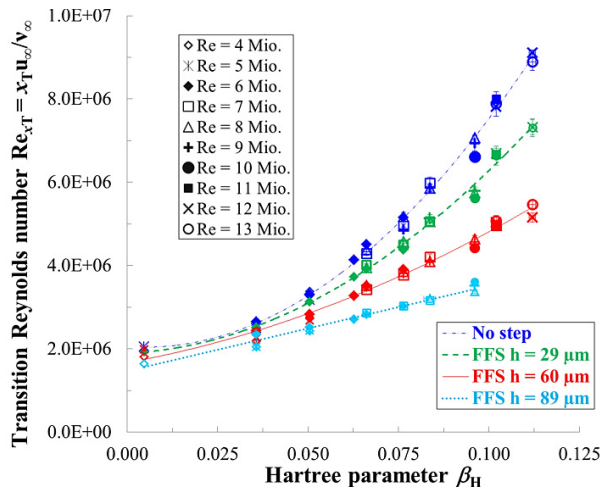
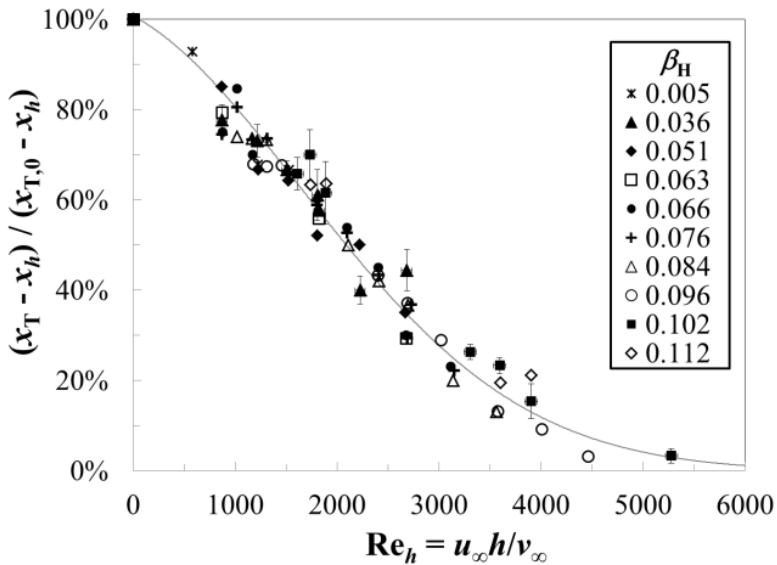


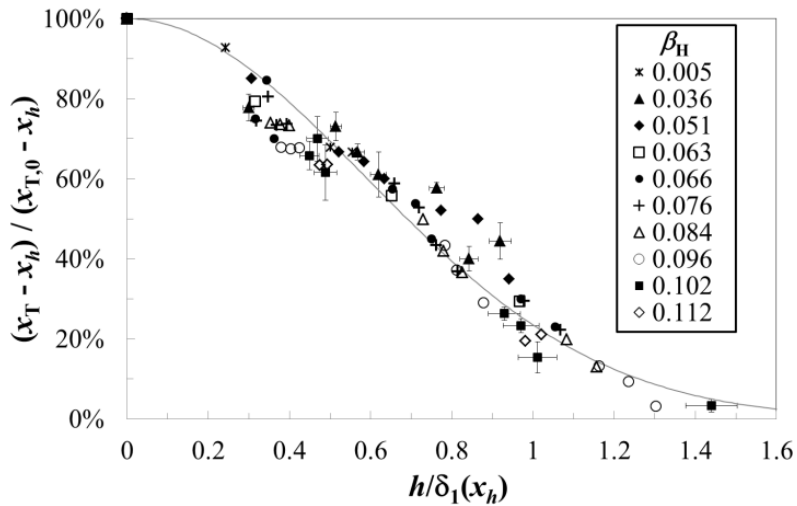
Fig. 5. Transition Reynolds number as a function of the streamwise pressure gradient for different configurations (with and without steps). $M = 0.77$, $T_w/T_{aw} \sim 1.045-1.065$. Polynomial approximations of the data sets for the different configurations (quadratic: smooth configuration and configurations with FFS of height $h = 29$ and $60 \mu\text{m}$; linear: configuration with FFS of height $h = 89 \mu\text{m}$) are also shown.

For these experiments, where the following was given: fluid stream, disturbance environment, pressure gradient, thermal condition at the model surface, position of the imperfection, and shape of the imperfection, the transition location x_T was a function only of the imperfection height h , the flow velocity u , and the fluid viscosity ν ³⁴. These four variables involve only the units of length and time: dimensional analysis tells us that the general functional relation between the four dimensional quantities can be reduced to a relation between two independent non-dimensional parameters. The non-dimensional parameter $s = (x_T - x_h)/(x_{T,0} - x_h)$ was chosen for the transition location: it expresses the relative change in transition location as reduced from its natural position $x_{T,0}$ to the step location x_h ¹⁴. One possible choice for the non-dimensional parameter containing the remaining variables is the step Reynolds number $Re_h = uh/\nu$. Although $u_e(x_h)$ and $\nu_e(x_h)$ at the boundary layer edge appear in general more appropriate³³, this non-dimensional parameter was formed in earlier work^{15,6} using u_{∞} and ν_{∞} ; since the differences between u_e and ν_e and the corresponding values in the freestream were small (the contour-induced variation in the velocity was small, as can be seen in the pressure distributions shown in Fig. 3), the freestream quantities could be also taken for the current analysis. The step Reynolds number $Re_h = u_{\infty}h/\nu_{\infty}$ is thus used in Fig. 6a to represent the experimental results as $(x_T - x_h)/(x_{T,0} - x_h)$ vs. Re_h . An alternative choice for the non-dimensional imperfection parameter is suggested by linear stability theory. Provided that transition occurs at some distance from the surface imperfection, the distortion in the velocity profile has disappeared, leaving only increased amount of disturbances as the primary effect of the imperfection. The contribution of the imperfection to the disturbance in the critical frequency range for which amplification occurs is considered to depend on its height relative to the boundary layer thickness^{34,35}. Guided by this physical concept, $h/\delta_1(x_h)$ ^{6,8} was selected as the second non-dimensional parameter, where $\delta_1(x_h)$ is the boundary layer displacement thickness computed at the step location $x_h/c = 35\%$ for the smooth configuration using COCO, see Section 2. It can be shown²² that δ_1 is not only a function of u and ν , but also of β_H and T_w/T_{aw} , and therefore appears to be a suitable parameter for investigations where these factors are changed. Moreover, $\delta_1(x_h)$ is clearly dependent on the step location, thus it can be expected that configurations with steps installed at different locations can be compared using the non-dimensional parameter $h/\delta_1(x_h)$. The relative variation in transition location $(x_T - x_h)/(x_{T,0} - x_h)$ is presented as a function of the relative step height $h/\delta_1(x_h)$ in Fig. 6b. It can be seen in Figs. 6a and 6b that plotting $(x_T - x_h)/(x_{T,0} - x_h)$ as a function of Re_h and $h/\delta_1(x_h)$ gave good correlation of the experimental data. The value of $s = (x_T - x_h)/(x_{T,0} - x_h)$ was observed to decrease at larger step Reynolds numbers and at larger non-dimensional step heights $h/\delta_1(x_h)$. Moreover, the correlations were shown to be practically independent of the investigated streamwise pressure gradients. This result is in agreement with the behavior found in previous studies on spanwise trip wires^{34,35} and steps^{6,8}, where a limited variation of the streamwise pressure gradient had been carried out. In fact,

pressure gradients are considered to mainly modify the stability of the base flow with almost no effect on the disturbance caused by the imperfection^{6,8-34,36}. This conclusion differs from that reported in Refs. 9-11 of a substantial stabilizing effect of flow acceleration that allows manufacturing requirements for a NLF surface to be loosened. Note that the available data⁹⁻¹¹ do not seem to clearly support such a conclusion. Nevertheless, it should be kept in mind that larger Hartree parameters maintain their favorable effect on transition in absolute sense, viz. on Re_{xT} , even in the presence of forward-facing steps, as shown in Fig. 5 of the current work. The best approximation of the present experimental data was provided by a Gaussian function, shown in Figs. 6a and 6b by a solid line.



a



b

Fig. 6. Relative change in transition location as a function of (a) the step Reynolds number Re_h and (b) the relative step height $h/\delta_1(x_h)$ for different streamwise pressure gradients. $M = 0.77$, $T_w/T_{aw} \sim 1.045\text{--}1.065$. Solid lines: Gaussian approximation. Note that the data below the approximation function in the range $0.3 \leq h/\delta_1(x_h) \leq 0.5$ were obtained at a wall temperature $T_w/T_{aw} \sim 1.06$ larger than that at which the smooth configuration was investigated $T_w/T_{aw} \sim 1.05$. Similarly, the data above the approximation function in the range $0.75 \leq h/\delta_1(x_h) \leq 0.95$ were obtained at a wall temperature $T_w/T_{aw} \sim 1.05$ lower than that at which the smooth configuration was investigated $T_w/T_{aw} \sim 1.055$. The deviation of these data from the main trend is due to this difference in the wall temperature ratio. The combination of the effects of forward-facing steps and a non-adiabatic surface will be discussed in a future publication.

Criteria for allowable tolerances for forward-facing steps on NLF surfaces can now be established from the obtained relations. For example, using the Gaussian approximation of the experimental results, a loss of laminarity $\Delta s = 10\%$ (corresponding to $(x_T - x_h)/(x_{T,0} - x_h) = 90\%$) is found at $Re_h = 600$ and $h/\delta_1(x_h) = 0.27$; $\Delta s = 20\%$ is found at $Re_h = 1030$ and $h/\delta_1(x_h) = 0.39$. Depending on the loss of laminarity Δs that can be permitted for a certain NLF surface, the corresponding values of Re_h and $h/\delta_1(x_h)$ can be determined.

The values of critical non-dimensional roughness parameters found in the present work are lower than those reported in the literature^{1,5,8}. Moreover, transition was observed to move gradually towards a more upstream location with increasing Re_h or $h/\delta_1(x_h)$, similarly to the behavior shown in Refs. 7 and 8, rather than abruptly as a certain critical value of non-dimensional imperfection parameter has been exceeded⁶. Interestingly, the critical values of $h/\delta_1(x_h)$ (or Re_h) and the functional relations found in the present work for forward-facing steps are closer to those reported in previous work on spanwise wires^{34,36} and backward-facing steps^{5,8}. The differences between the current results and those reported in the literature can be related to differences in one or more of the following factors:

- Shape of the step (in streamwise¹ and spanwise direction).
- Investigated stability situation: smooth configuration with an uniform pressure gradient^{7,8} or with transition occurring over a region of adverse pressure gradient preceded by a region of favorable pressure gradient^{1,6}.
- Criterion to define the critical step height, i.e. non-dimensional roughness parameter at which the extent of laminar area is reduced below a certain threshold.
- Measurement technique used to measure transition: thermographic method (infrared thermography⁶, TSP in the present work), sublimating chemicals¹, hot-wire⁷, Preston tube⁸ and flattened Pitot tube⁶. Information about the transition front in the spanwise direction is available only in Refs. 1 and 6.
- Disturbance environment. (Wind tunnel turbulence in the presence of spanwise wires was however observed to have small influence on the relation between $Re_{xT}/Re_{xT,0}$ and relative step height³⁴.)

In Ref. 1, sharp forward-facing steps were investigated only at large step Reynolds numbers $Re_h \geq 2720$, and transition was found at the step location in all considered cases. Information about one or more of the above factors is not available in Refs. 5-8. It should be emphasized here that no information at all is available about the experiments conducted to develop the criterion reported in Ref. 5.

4. Conclusions

Studies of the effect of forward-facing steps on boundary layer transition were successfully carried out at the DNW-KRG wind tunnel facility by means of the Temperature-Sensitive Paint measurement technique. The experimental setup allowed the independent variation of step height, chord Reynolds number, and streamwise pressure gradient, and thus the systematic investigation of the effect of these parameters on boundary layer transition. Chord Reynolds numbers up to 13 Mio., approximately zero and favorable pressure gradients in the range of Hartree parameters $0.005 \leq \beta_H \leq 0.112$, and forward-facing steps of relative height up to $h/\delta_1(x_h) \sim 1.45$ (corresponding to step Reynolds numbers $Re_h \leq 5300$) were examined at a Mach number $M = 0.77$. Even the smallest forward-facing steps studied in this work were found to shift the transition location to a more upstream position. Transition was observed to move gradually towards the step location with increasing step Reynolds number Re_h and increasing relative step height $h/\delta_1(x_h)$. The surface imperfections were shown to have a negligible effect on the pressure distributions, except the region around the step location. The transition Reynolds number at a given combination of step height and streamwise pressure gradient was seen to be practically independent of the chord

Reynolds number. At fixed chord Reynolds number and model configuration, the effect of larger flow acceleration was to delay transition. A favorable effect of larger Hartree parameters on boundary layer transition was found also in the presence of forward-facing steps; the increase in transition Reynolds per change in Hartree parameter was, however, less pronounced in the presence of higher steps. Moreover, the reduction in transition Reynolds due to the effect of the surface imperfection was observed to be more marked at larger Hartree parameters, according to the increased sensitivity of transition to the forward-facing steps for the considered stability situations. Non-dimensional parameters were used to represent the effect of the surface imperfections on boundary layer transition. The plots of the relative change in transition location $s = (x_T - x_h)/(x_{T,0} - x_h)$ as a function of the step Reynolds number Re_h and of the relative step height $h/\delta_1(x_h)$ gave good correlation of the results. The correlations were found to be practically independent of the streamwise pressure gradient in the examined range of Hartree parameters. Criteria for the allowable tolerances on low-sweep NLF surfaces, where growth of Tollmien-Schlichting instabilities is the predominant mechanism leading to transition to turbulence, can now be derived from the functional relations determined in this work.

Acknowledgements

The authors would like to thank: S. Hein (DLR) for the assistance during the definition of the tests and the analysis of the results and for the modification of COCO for computations with isothermal wall; C. Fuchs and T. Kleindienst (DLR) for the constant support during the preparation of the model; S. Koch (DLR) for the assistance during the experimental campaign and the evaluation of the results; U. Henne and W. E. Sachs (DLR) for the help in the TSP data analysis; W. H. Beck (DLR) for the productive discussions of the results; L. Schojda and U. G. Becker (DLR) for the support during the model design phase; V. Ondrus (University of Hohenheim) for the chemical development of the Temperature-Sensitive Paint; R. Kahle, M. Aschoff, and S. Hucke (DNW-KRG) for the support during the whole test campaign; L. Koop and H. Rosemann (DLR) for the constant advice during the definition and conduction of this project; S. Schaber (Airbus) for his suggestions during model preparation; U. Fey (DLR) and Y. Egami (Aichi Institute of Technology) for the work on the development of the TSP measurement technique at DLR in the last decade; W. Schröder (RWTH Aachen), A. Dillmann (DLR), W. Kühn, and G. Schrauf (Airbus) for their invaluable advice.

References

- Holmes BJ, Obara CJ, Martin GL, Domack CS. Manufacturing Tolerances for Natural Laminar Flow Airframe Surfaces. SAE Paper No. 850863, 1985.
- Nayfeh AH. Influence of Two-Dimensional Imperfections on Laminar Flow. SAE Paper No. 921990, 1992.
- Rizzetta DP, Visbal MR. Numerical Simulation of Excrescence Generated Transition. AIAA Paper No. 2013-0079, 2013.
- Fage A. The Smallest Size of a Spanwise Surface Corrugation which affects Boundary-layer Transition. R&M No. 2120, 1943.
- Nenni JP, Gluyas GL. Aerodynamic design and analysis of an LFC surface. *Astronautics and Aeronautics*, 1966; p. 52–7.
- Perraud J. Laminar-turbulent transition on aerodynamic surfaces with imperfections. RTO-AVT-111, 2004.
- Wang YX, Gaster M. Effect of surface steps on boundary layer transition. *Exp. Fluids* 2005; **39**: 679–86.
- Crouch JD, Kosorygin VS, Ng LL. Modeling the effects of steps on boundary layer transition. 6th IUTAM Symposium on Laminar-Turbulent Transition, Bangalore, India, 2006.
- Bender AM, Elliott JR, Shinagawa Y, Korntheuer AJ, Drake A, Westphal RV, Gerashchenko S, McKeon BJ, Yoshioka S. An Approach to Measuring Step Excrescence Effects in the Presence of a Pressure Gradient. AIAA Paper No. 2010-0373, 2010.
- Gerashchenko S, McKeon BJ, Westphal RV, Bender AM, Drake A. Hot-Wire Measurements of the Influence of Surface Steps on Transition in Favorable Pressure Gradient Boundary Layers. AIAA Paper No. 2010-374, 2010.
- Drake A, Bender AM, Korntheuer AJ, Westphal RV, McKeon BJ, Gerashchenko S, Rohe W, Dale G. Step Excrescence Effects for Manufacturing Tolerances on Laminar Flow Wings. AIAA Paper No. 2010-375, 2010.
- Edelmann CA, Rist U. Impact of forward-facing steps on laminar-turbulent transition in transonic flows without pressure gradient. AIAA Paper No. 2013-0080, 2013.
- Duncan Jr. GT, Crawford BK, Tufts MW, Saric WS, Reed HL. Effects of Step Excrescences on Swept-Wing Transition. AIAA Paper 2013-2412.
- Duncan Jr. GT, Crawford BK, Tufts MW, Saric WS, Reed HL. Effects of Step Excrescences on a Swept Wing in a Low-Disturbance Wind Tunnel. AIAA Paper 2014-0910, 2014.
- Holmes BJ, Obara CJ, Yip LP. Natural Laminar Flow Experiments on Modern Airplane Surfaces. NASA TP 2256, 1984.
- Schrauf G. Status and Perspectives of Laminar Flow. *Aeronautical J.* 2005; **109 (1102)**: p. 639–44.

17. Kruse M, Wunderlich TF, Heinrich L. A Conceptual Study of a Transonic NLF Transport Aircraft with Forward Swept Wings. AIAA Paper No. 2012-3208, 2012.
18. Rosemann H. The Cryogenic Ludwig-Tube Tunnel at Göttingen. AGARD-R-812; Cologne, Germany; 1996. p. 8-1 to 8-13.
19. Koch S. Zeitliche und räumliche Turbulenzentwicklung in einem Rohrwindkanal und deren Einfluss auf die Transition an Profilmodellen. DLR-FB-04-19, 2004.
20. Costantini M, Hein S, Henne U, Klein C, Koch S, Sachs WE, Schojda L, Rosemann H, Koop L, Ondrus V. The effect of pressure gradient and a non-adiabatic surface on boundary layer transition investigated by means of TSP. AIAA Paper No. 2013-1137.
21. Arnal D. Boundary Layer Transition: Prediction, Application to Drag Reduction. AGARD Report No. 786, 1992, p. 5-1 to 5-59.
22. Schlichting H, Gersten K. *Boundary-Layer Theory*. 8th ed., Springer-Verlag, Berlin Heidelberg, 2000.
23. Costantini M, Fey U, Henne U, Klein C. Influence of non-adiabatic model surface on transition measurements using the Temperature-Sensitive Paint technique in a cryogenic wind tunnel. AIAA Paper No. 2012-2830, 2012.
24. Liu T, Sullivan JP. *Pressure and Temperature Sensitive Paint*. Springer-Verlag; Berlin Heidelberg; 2005.
25. Tropea C, Yarin AL, Foss JF (eds.), *Springer Handbook of Experimental Fluid Mechanics*, Springer-Verlag, Berlin Heidelberg, 2007, Chap. 7.4: Transition-Detection by Temperature-Sensitive Paint.
26. Fey U, Egami Y, Engler R. High Reynolds Number Transition Detection by means of Temperature-Sensitive Paint. AIAA Paper No. 2006-0514, 2006.
27. Streit T, Horstmann KH, Schrauf G, Hein S, Fey U, Egami Y, Perraud J, El Din IS, Cella U, Quest J. Complementary Numerical and Experimental Data Analysis of the ETW Telfona Pathfinder Wing Transition Tests. AIAA Paper No. 2011-0881, 2011.
28. Meyer F, Kleiser L. Numerical Investigation of Transition in 3D Boundary Layers. AGARD-CP-438; Cesme, Turkey; 1988. p. 16-1 to 16-17.
29. Schrauf G. COCO – A Program to Compute Velocity and Temperature Profiles for Local and Nonlocal Stability Analysis of Compressible, Conical Boundary Layers with Suction. ZARM Technik Report, 1998.
30. Hein S. Priv. comm., 2013.
31. Redeker G, Mueller R, Blanchard A, Reneaux J. Evaluation of Transonic Laminar Airfoil Tests under Cryogenic Conditions Including Stability Analysis and Computational Results. Proceedings of the DGLR/AAAF/RAeS 1st European Forum on Laminar Flow Technology, Hamburg, Germany, 1992, p. 141–51.
32. Schrauf G. LILO 2.1 – Users Guide and Tutorial. GSSC Technical Report 6, 2006.
33. Forte M, Perraud J, Gentili L, Casalis G. Experimental and numerical study of the effect of gaps on laminar turbulent transition of incompressible boundary layers. 8th IUTAM Symposium on Laminar-Turbulent Transition, Rio de Janeiro, Brazil, 2014.
34. Dryden HL. Review of published data on the effect of roughness on transition from laminar to turbulent flow. *J. Aero. Sci.* 1953; **20 (7)**: p. 477-82.
35. Tani I. Effect of Two-Dimensional and Isolated Roughness on Laminar Flow. In: Lachmann GV (ed.). *Boundary Layer and Flow Control*, Vol. 2, Pergamon Press, 1961, p. 637-56.
36. Smith AMO. A Discourse on Roughness, Turbulence and Noise and What Is Known About Their Effects on Transition. Part 1. Allowable Values of Discrete Roughness, Continuous Roughness and Waviness. DTN-7802-7A, 1979.